Noncontact optical displacement measurements by dynamic contrast auto focusing for slow oscillatory motion

Evgeniy Makagon,[a,†,*] **Sergey Khodorov**,[a,†] **Anatoly Frenkel**,[b,c] **Leonid Chernyak**,[d] **and Igor Lubomirsky**[a]

[a]Weizmann Institute of Science, Department of Materials and Interfaces, Rehovot, Israel
[b]Brookhaven National Laboratory, Upton, New York, United States
[c]Stony Brook University, Department of Materials Science and Chemical Engineering, Stony Brook, New York, United States
[d]University of Central Florida, Department of Physics, Orlando, Florida, United States

Abstract. A noncontact displacement system suitable for tracking slow moving surfaces with low reflectivity is demonstrated. The displacement is measured by dynamic tracking of the moving focal plane of the sample under test. The system comprises a camera, a vertical digital piezo driver, and a data acquisition module. The tracking effect is achieved by continuously driving the sample with a 2-μm sweep around the focal plane, simultaneously acquiring the sample position and images of the part of the sample defined as a region of interest (ROI). The position of the focal plane is identified by fitting the contrast of the ROI versus the stage position to a Gaussian function. Using an ROI provides the ability to test various regions across the object and eliminates the demand for the surface to be flat or reflective. The system is low cost, is applicable to a large variety of samples and has an accuracy better than 10 nm. © *2021 Society of Photo-Optical Instrumentation Engineers (SPIE)* [DOI: 10.1117/1.OE.60.12.124112]

Keywords: contrast auto focusing; displacement measurement; slow oscillatory motion.

Paper 20210921 received Aug. 19, 2021; accepted for publication Dec. 7, 2021; published online Dec. 29, 2021.

1 Introduction

Displacement measurements are in great demand for various scientific and industrial purposes.[1–4] While some methods such as push-rod dilatometry and scanning probe microscopy require physical contact with the surface under testing, noncontact methods are often preferred for measurements of sub-mm size objects. Noncontact displacement sensing is typically based on capacitive,[5,6] inductive,[7] or optical sensors.[3,8–13] Capacitive and inductive methods work with electrically conductive surfaces, which restricts the variety of samples that can be handled by these methods. Moreover, both inductive and capacitive sensors have to be positioned in close proximity to the surface. Hence, they may suffer from poor stability because small fluctuations of the sample's temperature render the measurements inaccurate. Furthermore, both techniques are based on application of an electric or magnetic field, which may be detrimental for the measurement accuracy of micro/nanoelectromechanical system devices.

Optical techniques for measuring distance/displacement do not require close proximity to the sample or a conductive surface and potentially can be very accurate. Optical sensing techniques vary widely from the simplest light intensity, optical fiber-based sensors to highly complex and expensive interferometric-based methods.[3,8–13] Most optical techniques currently in use require expensive laser equipment, reflective surfaces, and a mechanically/thermally stable environment. The latter requirements are especially critical for slow moving surfaces because most of the thermal drift noise occurs at low frequencies. Although there is a considerable amount of commercial and academic literature describing laboratory systems that reliably deal with monitoring

*Address all correspondence to Evgeniy Makagon, evgeniy.makagon@weizmann.ac.il

†Equal contribution

relatively rapid displacements (μm/s), the range of a <0.1 μm/s is not covered. In this view, a simple noncontact method to monitor slow displacement of poorly reflective surfaces may be beneficial for a range of applications.

Recent advances in the piezoelectric-driven stages, providing highly reproducible positioning with an accuracy better than 5 nm, opened new possibilities for constructing displacement monitoring systems for MEMS. In this report, we describe a simple white light-based noncontact system operating on a dynamic focus detection principle to monitor displacement. The apparatus comprises three components: a camera, a high-accuracy (4 nm) vertical piezoelectric positioner (stage), and a data collection module to track the focal plane of the device under test.

Previously described focus detection-based distance measurement techniques require lattice pattern projection on the surface of the subject under test as a focus assisting mechanism.[14,15] The method described here uses the image of the natural surface and does not require the surface under investigation to be reflective nor does it impose limitations on surface shape and geometry. Moreover, the described apparatus, through its novel design, allows for precise position tracking of a moving surface rather than distance measurement of a stationary surface as has been reported thus far.[16–18] The system can be implemented with relatively inexpensive components. It has a short stabilization time and can conduct displacement measurements of samples with <10 nm resolution.

2 Description of the Experimental Setup

The noncontact displacement measurement system and its components are depicted in Fig. 1. The sample (1 and inset) is mounted on a XYZ piezo stage (PI-Physik Instrumente GmbH & Co.) (2), equipped with a manual position adjusting unit (3).

The sample is connected to an arbitrary waveform generator (DG4102, Rigol) and a high precision source measuring unit (B2901A, Keysight) functioning as a multimeter. A high power

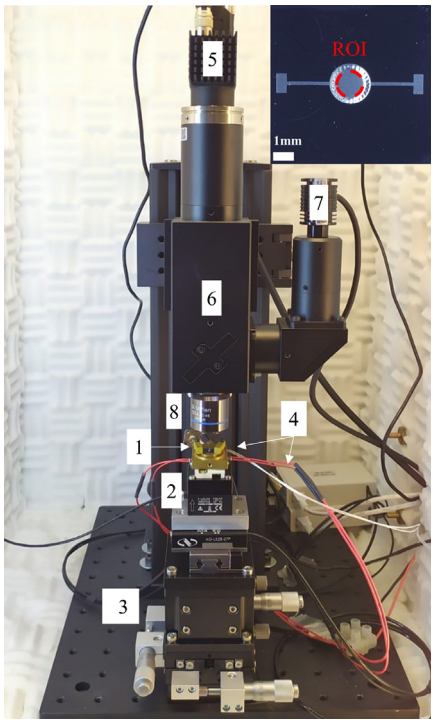

Fig. 1 Detailed scheme of the measuring system and its components: (1) Sample. (2) XYZ piezo stage. (3) Manual adjustment unit. (4) High power-resistive heating elements (red wires) and Pt-resistive temperature sensor (silver wire). (5) CMOS camera. (6) Microscope unit (beam splitter with a lens stack). (7) 5000K LED light source. (8) 50× objective lens. Inset: top surface of the sample depicting the ROI relevant for measurement.

resistive heating power supply and temperature controller are implemented inside the sample holder (PTC10, Stanford Research Systems) (4). A camera (Sony IMX273 CMOS sensor 1456×1088, 12 bit, 165 f/s, dynamic range: 72 dB) (5) is mounted on a custom-made microscope unit (6) equipped with a 5000-K led light source (7) and a 50×, long working distance (18 mm) infinity corrected objective (SLMPlan 50, Olympus) (8). A piezo stage controller (E-709 nanopositioning piezo controller, PI-Physik Instrumente GmbH & Co.) is connected to a multichannel data acquisition module (DAQ-USB-6000, NI-National Instruments) for real-time stage position recording. The piezo-stage trigger is connected to the acquisition module and the camera to ensure simultaneous data recording. The whole system is mounted in a thermally insulated box to minimize temperature fluctuation.

3 Principle of Operation

The algorithm [Fig. 2] utilizes a traditional contrast-based autofocusing principle often used for static objects[17] and adds a dynamic focus-tracking capability via a continuous scan around the focal point.

To identify the focal point of a continuously moving surface, the stage with the object of interest mounted on it, is driven back and forth in a 2 μm range around the initial focal point. The position of the piezo stage is continuously recorded [Fig. 3(a)], while the camera simultaneously acquires continuous grayscale images of the object: 70 frames per 2 μm of the vertical movement of the stage. The contrast of a selected segment of the image that is of interest for investigation is calculated for each frame (C_k) from the pixel variance of the grayscale brightness (P_{ij}):

$$C_k = \sum \frac{\sum_{i,j=1}^{n} (P_{ij} - \overline{P})^2}{(n-1) \cdot \overline{P}}, \tag{1}$$

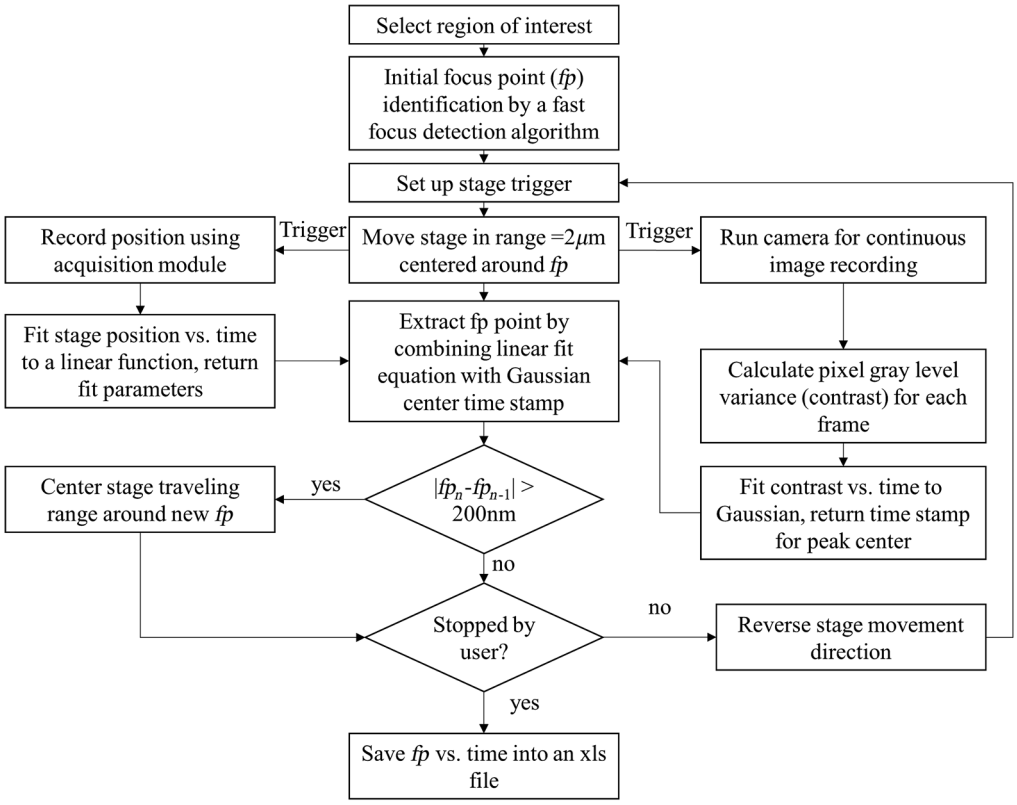

Fig. 2 Detailed description of the dynamic focus-tracking algorithm.

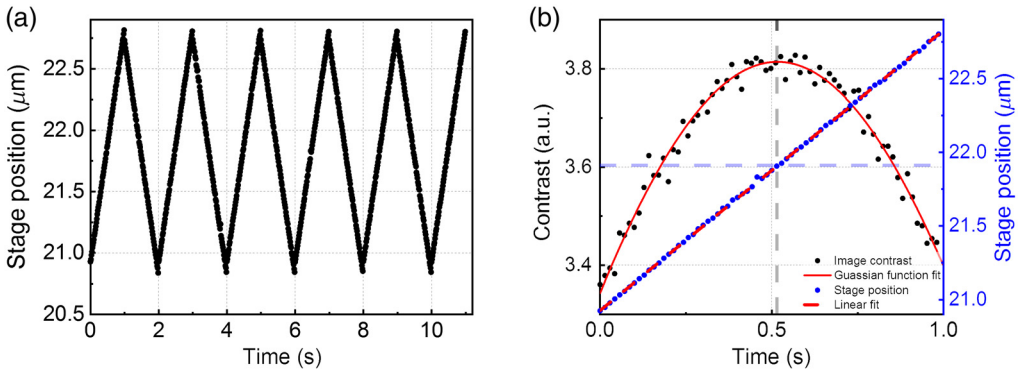

Fig. 3 Dynamic focus tracking: (a) A segment of the continuous periodic stage movement recorded by the data acquisition module. The stage is driven periodically and travels 2 μm per second, during which 70 frames of the sample's surface image are recorded by the camera. The contrast of each frame is calculated [Eq. (1)]. (b) Focal point detection: the position of the stage and the calculated image contrast are shown as a function of time for a single stage travel. The dependence of the contrast on time is fitted to a Gaussian function [Eq. (2)], the center of which is the time at which the focal point was identified (gray-dashed line). The position of the stage at the time corresponding to the center of the Gaussian (blue-dashed line) is deduced by fitting the dependence of the stage position on time to a linear regression (red-dashed line) [Eq. (3)].

where $\overline{P}$ is the average value of P_{ij}, n is the number of pixels in the image, and k is the frame number. The dependence of the contrast on time is fitted to a Gaussian function ($C(t)$), the center of which is interpreted as the focal point (μ):

$$C_{k=1-70}(t) = ae^{\frac{(t-\mu)^2}{\sigma^2}}, \tag{2}$$

where $\mu = 0.516 \pm 0.005$s in Fig. 3(b) is an example (gray-dashed line). σ defines the full-width half-maximum of the Gaussian function.

The dependence of the stage position on time is fitted to a linear regression, giving an exact stage position at a given time ($z(t)$). The absolute position of the focal plane ($z(\mu)$) is deduced from the time, at which the Gaussian fit of the contrast reaches maximum [$t = \mu$, blue-dashed line in Fig. 3(b)]:

$$z(t) = a \cdot t + b \overset{t=\mu}{\Rightarrow} z(\mu) = a \cdot \mu + b. \tag{3}$$

To obtain a reliable tracking of the sample position, the movement of the sample has to be less than 1/50 of a single sweep length (2 μm). Considering the manufacturer recommended stage sweep velocity of 2 μm/s, the system is applicable for the objects moving slower than 0.08 μm/s. When measuring periodic signals, the best results are achieved with sampling at a frequency that is at least 50 times higher than that of the sample. For the example shown in Sec. 4, a 700-mHz sampling frequency was used for monitoring a sample oscillating at $<$ 35 mHz. The initial focal position is brought manually to the mid-range (25 out of 50 μm) of the stage, and the initial focal point is roughly estimated by a fast focus detection algorithm described below. The stage is swept $\approx$10 μm around the manually set focal point with a step size of 50 nm determining the contrast of the images at each step.

To minimize thermal fluctuations, the system is mounted in a cabinet with the inner walls covered by a sound absorbing foam. Efficient thermal insulation, however, implies that the system will undergo thermal equilibration (up to 90 min), during which the focal point may drift by up to 5 μm [Fig. 4(a)]. Once the thermal equilibrium of the measurement system with the box is reached, the thermal drift has standard deviation of 7 nm over the 2 h [Fig. 4(b)]. This is despite the fact that the temperature outside the box fluctuated more than 3°C.

The accuracy of the measurement strongly depends on the quality of the Gaussian fit of the "contrast – time" dependence [Fig. 3(b)]. Most accurate results were achieved when the

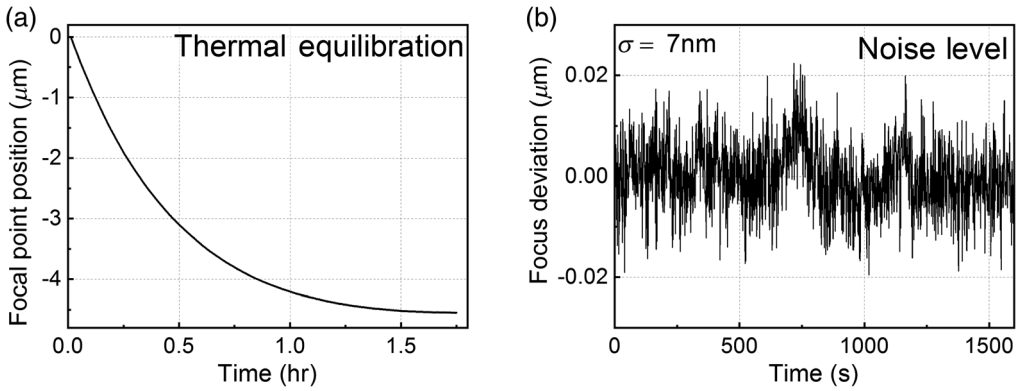

Fig. 4 Thermal equilibration and noise level: (a) focal point position as a function of operation time. The focal point changes significantly during the first hours of operation due to equipment thermal equilibration. (b) Focal point position deviation from the mean value after equilibration period. The standard deviation of the noise is 7 nm.

Gaussian profile was centered in the sweeping window, which, for the samples used for this study [Sec. 4], is 2 μm. To maintain the sweeping window centered on the focal point, each time the focal point shifted beyond 10% of the sweeping range, the sweeping range was shifted accordingly.

During the measurements, the contrast value is calculated over a certain region of interest (ROI) of the acquired images. The size of the ROI may range from tens to thousands of pixels of the image. Selection of the ROI is based on two considerations. (1) With a sufficiently large ROI, the points with outlying values of brightness (both low and high) are smoothed out, making the result much more reliable with respect to small area-based techniques, such as interferometry or scanning probe microscopy. (2) By selecting different ROIs, different areas of the samples can be probed. Thus, the system can work with the samples exhibiting nonuniform displacement. In this view, the ROI can provide an average displacement over a whole sample or probe different parts of it.

4 Experimental Verification

The system was tested with the electrochemomechanical (ECM) devices described in Ref. 19: thin film self-supported structures that are 2 mm in diameter and 2 μm thick [Fig. 1 inset]. Electric bias forces the opposite surfaces (top and bottom) to undergo expansion/contraction, forcing the structure to bend with a characteristic response time of ≈10s. Bending causes maximum displacement in the center, while the edges remain clamped.

Therefore, the ROI was selected in the center of the sample (150 × 150 pixels) [Fig. 1 inset], where the displacement was approximately uniform. An alternating electric bias of 8 V at 10 mHz [red line in Fig. 5(a)] resulted in periodic displacement of ≈0.6 μm, easily traced by the measurement system. The magnitude of the displacement was independently verified with SPM and both values were found to be in good agreement, proving the viability of the method. The system remains reliable upon heating to at least 60°C, with no significant increase in the thermal equilibration time [Fig. 5(b)].

5 Conclusions

A noncontact displacement system suitable for tracking slow moving surfaces with low reflectivity is demonstrated. The displacement is measured by dynamic tracking of the moving focal plane of the sample under test. The system comprises a camera, a vertical digital piezoelectric positioner (stage), and a data acquisition module. The tracking effect is achieved by continuously driving the sample with a 2-μm sweeping range around the focal plane, simultaneously acquiring the sample position and images of the sample surface and compensating for mechanical or

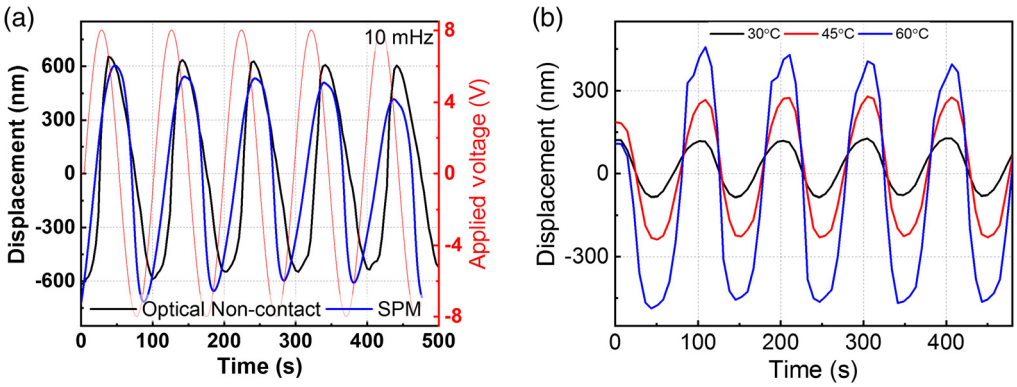

Fig. 5 Displacement measurements of electromechanical sample: (a) Room temperature measurements at 10 mHz 8V AC driving voltage (red line). The noncontact dynamic autofocusing system (black line) is compared with scanning probe microscopy measurements (blue line). (b) Temperature-dependent measurements at 10-mHz 8V AC driving voltage: 30°C (black line), 45°C (red line), and 60°C (blue line). Baseline subtraction was performed on all signals to allow for proper comparison.

thermal drifts. The position of the focal plane is identified according to a contrast-based focus detection algorithm. The system is low cost and can be used with a large variety of samples as it does not require specific surface geometry/morphology or close proximity to the surface. Selection of an ROI provides the ability to measure several regions at once and use selective area averaging, offering a wide dynamic range capable of measuring displacements of 20 nm to 10 μm with an accuracy better than 10 nm.

Acknowledgments

This work was supported by NATO Science for Peace award G5453, and, in part, by the BioWings project, which has received funding from the European Union's Horizon 2020 under the Future and Emerging Technologies (FET) program with Grant Agreement No. 801267. IL and AIF acknowledge the NSF-BSF program Grant No. 2018717. AIF acknowledges the support by NSF DMR Grant No. 1911592. The authors declare that there are no conflicts of interest.

References

1. D. J. Bell et al., "MEMS actuators and sensors: observations on their performance and selection for purpose," *J. Micromech. Microeng.* **15**(7), S153–S164 (2005).
2. J. Fraden, *Handbook of Modern Sensors*, Springer, New York (2010).
3. R. Leach, *Fundamental Principles of Engineering Nanometrology*, 2nd ed., William Andrew Publishing, Boston, Massachusetts (2014).
4. J. S. Wilson, *Sensor Technology Handbook*, Elsevier, Burlington (2004).
5. L. K. Baxter and R. J. Herrick, *Capacitive Sensors: Design and Applications*, IEEE Press, New York (1997).
6. A. J. Fleming, "A review of nanometer resolution position sensors: operation and performance," *Sens. Actuators A* **190**, 106–126 (2013).
7. M. R. Nabavi and S. N. Nihtianov, "Design strategies for eddy-current displacement sensor systems: review and recommendations," *IEEE Sens. J.* **12**(12), 3346–3355 (2012).
8. M. C. Amann et al., "Laser ranging: a critical review of unusual techniques for distance measurement," *Opt. Eng.* **40**(1), 10–19 (2001).
9. P. Girao et al., "An overview and a contribution to the optical measurement of linear displacement," *IEEE Sens. J.* **1**(4), 322–331 (2001).
10. H. Golnabi and P. Azimi, "Design and operation of a double-fiber displacement sensor," *Opt. Commun.* **281**(4), 614–620 (2008).

11. P. Hariharan, *Basics of Interferometry*, 2nd ed., pp. 1–226, Academic Press, San Diego, California (2007).
12. H. J. Jordan, M. Wegner, and H. Tiziani, "Highly accurate non-contact characterization of engineering surfaces using confocal microscopy," *Meas. Sci. Technol.* **9**(7), 1142–1151 (1998).
13. A. Shimamoto and K. Tanaka, "Geometrical analysis of an optical fiber bundle displacement sensor," *Appl. Opt.* **35**(34), 6767–6774 (1996).
14. H. Yoshida, "Focus detecting method, focus detecting mechanism and image measuring device having focus detecting mechanism," Mitutoyo Corp., Japan (2004).
15. T. Yoshizawa et al., "Displacement measurement by the detection of contrast variation of a projected pattern," *Proc. SPIE* **1756**, 82–85 (1993).
16. K. Kubo, "In-focus detection method and method and apparatus using the same for non contact displacement measurement," Mitutoyo Corporation, Tokyo, Japan (1995).
17. Y. Nakagawa and S. K. Nayer, "Method of detecting solid shape of object with autofocusing and image detection at each focus level," Hitachi Ltd., Japan (1990).
18. K. Ariga and K. Komatsu, "Method and apparatus for visual measurement" (2000).
19. E. Makagon et al., "All-solid-state electro-chemo-mechanical actuator operating at room temperature," *Adv. Funct. Mater.* **31**, 2006712 (2021).

Biographies of the authors are not available.